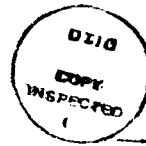


REPORT DOCUMENTATION PAGE

1a. AD-A231 672			1b. RESTRICTIVE MARKINGS												
2b. DECLASSIFICATION / DOWNGRADING			3. DISTRIBUTION / AVAILABILITY OF REPORT Approved for public release; distribution unlimited												
4. PERFORMING ORGANIZATION REPORT NUMBER(S) Technical Report # 57			5. MONITORING ORGANIZATION REPORT NUMBER(S)												
6a. NAME OF PERFORMING ORGANIZATION Dept. of Chemistry George Washington Univ.		6b. OFFICE SYMBOL (if applicable)	7a. NAME OF MONITORING ORGANIZATION Office of Naval Research (S 418)												
6c. ADDRESS (City, State, and ZIP Code) Washington, DC 20052		7b. ADDRESS (City, State, and ZIP Code) Chemistry Program 800 N. Quincy Street Arlington, VA 22217													
8a. NAME OF FUNDING / SPONSORING ORGANIZATION Office of Naval Research		8b. OFFICE SYMBOL (if applicable)	9. PROCUREMENT INSTRUMENT IDENTIFICATION NUMBER Contract N00014-89-J-1103												
8c. ADDRESS (City, State, and ZIP Code) Chemistry Program 800 Nth, Quincy, Arlington, VA 22217		10. SOURCE OF FUNDING NUMBERS <table border="1"><tr><td>PROGRAM ELEMENT NO.</td><td>PROJECT NO.</td><td>TASK NO.</td><td>R & T</td><td>WORK UNIT ACCESSION NC</td></tr><tr><td></td><td></td><td>01</td><td>34043</td><td></td></tr></table>				PROGRAM ELEMENT NO.	PROJECT NO.	TASK NO.	R & T	WORK UNIT ACCESSION NC			01	34043	
PROGRAM ELEMENT NO.	PROJECT NO.	TASK NO.	R & T	WORK UNIT ACCESSION NC											
		01	34043												
11. TITLE (Include Security Classification) Evidence for Vertical C ₂ on Ni as a Precursor for Graphite Nucleation (Unclassified) 2															
12. PERSONAL AUTHOR(S) David E. Ramaker															
13a. TYPE OF REPORT Interim Technical		13b. TIME COVERED FROM TO		14. DATE OF REPORT (Year, Month, Day) January 1991											
				15. PAGE COUNT 15											
16. SUPPLEMENTARY NOTATION Prepared for publication in Applications in Surface Science															
17. COSATI CODES <table border="1"><tr><th>FIELD</th><th>GROUP</th><th>SUB-GROUP</th></tr><tr><td></td><td></td><td></td></tr></table>			FIELD	GROUP	SUB-GROUP				18. SUBJECT TERMS (Continue on reverse if necessary and identify by block number) Carbides Nucleations Electron energy ion Graphite X-Ray absorption						
FIELD	GROUP	SUB-GROUP													
19. ABSTRACT (Continue on reverse if necessary and identify by block number) We interpret previously published C K edge CEELS and NEXAFS data for carbon Ni between 500-700K. The C K CEELS data for CO/Ni at 500K reveal the presence of C-C bonding on the surface, i.e. horizontal C _n (n=2,3...). The CEELS data for carbon at 620K reveal that some of the C ₂ species flip up at this temperature, while the others dissociate. Evidence for vertical C ₂ is seen only at higher carbon coverages, suggesting that some of the C ₂ are forced to flip up to make room for neighboring horizontal C ₂ 's to dissociate. These vertical C ₂ 's then apparently serve as the precursor for the nucleation of graphite, as it explains the lack of graphite formation at lower coverages when total dissolution into the bulk occurs. These results confirm recent effective medium theory calculations, which indicate that a nucleation step must be involved in the carbide to graphite transformation, and suggest that vertical C ₂ may be a precursor to this nucleation step on Ni. 91 2 04 097															
20. DISTRIBUTION / AVAILABILITY OF ABSTRACT <input checked="" type="checkbox"/> UNCLASSIFIED/UNLIMITED <input checked="" type="checkbox"/> SAME AS RPT. <input type="checkbox"/> DTIC USERS			21. ABSTRACT SECURITY CLASSIFICATION Unclassified												
22a. NAME OF RESPONSIBLE INDIVIDUAL Dr. Mark Ross			22b. TELEPHONE (Include Area Code) (202) 696-4409		22c. OFFICE SYMBOL										



OFFICE OF NAVAL RESEARCH

Contract N00014-89-J-1103

R & T Code 4134043-01

Technical Report No. 57

Accession For	
NTIS GRA&I	<input checked="" type="checkbox"/>
DTIC TAB	<input type="checkbox"/>
Unannounced	<input type="checkbox"/>
Justification	
By _____	
Distribution/	
Availability Codes	
Dist	Avail and/or Special
A-1	

Evidence for Vertical C on Ni₂
as a Precursor for Graphite Nucleation

By

DAVID E. RAMAKER

Prepared for Publication

in

Applications in Surface Science

George Washington University
Department of Chemistry
Washington, D.C.

January, 1991

Reproduction in whole or in part is permitted for
any purpose of the United States Government

* This document has been approved for public release
and sale; its distribution is unlimited.

Carbon is relatively unreactive with Ni. Thus Ni forms a relatively unstable carbide, which above 670K either undergoes dissolution into the bulk or at higher coverages forms a graphitic layer which sits high above the surface (e.g. 2.8 Å above a Ni(111) surface) [1]. Carbon is usually deposited on the surface by exposure to CO, ethylene, or acetylene. These molecular species decompose with heating, so that above 450K, SIMS data reveals all H and O has left the surface, leaving only C on the surface [2]. NEXAFS (near edge x-ray absorption fine structure) data have been very helpful in determining the various orientations of the molecular fragments below 450 K [3,4], but little new information from NEXAFS data has been reported for C/Ni above 450 K. In this work we utilize previously published [5,6] CEELS (core electron energy loss spectroscopy) and NEXAFS data [7] to obtain experimental verification that vertical C₂ acts as a precursor for graphite nucleation on Ni. Comparison is made with the NEXAFS technique commonly utilized below 450K.

1. NEXAFS results below 450K

The expression for the differential cross section derived for a transition from an s initial state (e.g. a C 1s state) to any π state can be written [4]:

$$\{1s \rightarrow \pi\} \propto (3\cos^2\beta - 1)(3\cos^2\theta - 1) + 2 \quad (1)$$

where θ is the angle between the surface normal and the electric field vector (or between the surface and the photon beam direction) and β is the angle between the surface normal and the molecular plane normal. A similar but approximate expression for excitation to a σ state can be written:

$$\{1s \rightarrow \sigma\} \propto (3\cos^2\alpha - 1)(3\cos^2\theta - 1) + 2. \quad (2)$$

Here α is the angle between the surface normal and the main molecular symmetry axis. When the ethylene is lying flat on the surface, α is 90° and β is 0°. In this case eqs. 1 and 2 reduce to $3\sin^2\theta$ and $6\cos^2\theta$. On the other hand, when the ethylene axis stands perpendicular to the surface, α is 0° and β is

90°. In this case, eqs. 1 and 2 reduce to $6\cos^2\theta$ and $3\sin^2\theta$, respectively. The latter more specific expressions are apparently qualitatively valid for most other molecules as well [7].

Fig. 1 summarizes the data [3,4] for ethylene on Pt(111) or Ni(100) at various temperatures and coverages. These data for all four adsorbed species reveal the characteristic π^*_{CC} and σ^*_{CC} peaks and the opposite variation with θ for nearly vertical and horizontal orientations of the adsorbates, as anticipated by eq. 1 and 2. We have given the initial bound state feature the label π^*_{CM} , in Fig. 1, i.e. carbon-metal antibonding rather than π^*_{CC} , since for most of the four cases this is more appropriate. These data were utilized previously to quantitatively determine the orientation angles for the four different adsorbate orientations on the surface [3,4]. Fig. 1 also shows our assignments for some of the smaller peaks such as the π^*_{CH} and σ^*_{CH} peaks as well as Rydberg or atomic-like np features. Our assignments are based on comparison with other NEXAFS data and theoretical calculations [8].

A combination of HREELS, NEXAFS, and PES data and theoretical calculations have been utilized to previously determine the orientation and bonding of ethylenic species to metal surfaces as schematically indicated in Fig. 1. For $C_2H_4/Pt(111)$ at 90K, the molecule is believed to be di- σ -bonded to the Pt surface, i.e. the molecule lies flat on the surface ($\alpha = 90^\circ$ and $\beta = 0^\circ$). Here the molecule is apparently only partially rehybridized, leaving the molecule somewhere between an sp^2 and sp^3 type structure. At 300K, Fig. 1b, the molecule stands erect ($\alpha = 0^\circ$ and $\beta = 90^\circ$) forming an ethylidyne species, i.e. sp^3 hybridized with 3 C-Pt bonds and 3 C-H bonds [3]. On Ni(100) at 130K, ethylene is π -bonded to the surface (i.e. more fully sp^3 hybridized); however, the molecule is not lying completely flat ($\alpha = 0^\circ$ and $\beta = 50^\circ$) [4]. Finally on Ni(100) at 180K, a more erect ($\alpha = 30^\circ$ and $\beta = 65^\circ$) vinyl species

is present [4]. The molecule is still essentially sp^2 hybridized, but a full σ C-M bond is formed in place of one C-H bond. In summary, the adsorbates at lower temperature lie more horizontal, those at higher temperature more vertical.

It is interesting to compare the peak energies for the more horizontal adsorbates with those for the more vertical. No significant energy shift in the σ^*_{CC} peak is evident, although this might have been expected particularly for ethynidyne (curve b) since the C-C bond is in this case a single σ bond. Note that the π^*_{CM} peak has higher energy for the more vertical adsorbates than for the horizontal. We believe this is because the adsorbate-metal bond is indeed stronger for the vertical adsorbates than for the horizontal adsorbates. We have reported a more detailed interpretation of these curves elsewhere [8].

2. CEELS above 450K

Above 450K, SIMS data reveal that all H and O has left the surface, leaving only C on the surface [2]. Recent calculations utilizing effective medium theory (EMT) [1] suggest however that further molecular orientation changes occur. In the EMT approach, the atom positions are determined by the electron density, each atom seeking its own unique optimum density. These calculations conclude that at intermediate coverage, the C-C interaction drives atoms closer to Ni, but in a graphite layer, the C-C interaction drives them away from the surface. They conclude then that the carbidic to graphite evolution is clearly discontinuous, so that a nucleation step must be involved. The calculations also suggest that a horizontal C_2 species on a Ni(111) surface is not stable at high temperature, but that a vertical (i.e. perpendicular) C_2 species may be stable on the Ni surface [1]. However, this vertical C_2 is too close to the surface to serve as a nucleation site for graphite formation by itself. Only a C_3 species moves sufficiently far from the metal surface to serve as a graphite nucleation site. Darling et al. [1] then postulate that a vertical C_2

species may either "tip over" to form a C_3 species, which moves away from the surface and forms a graphite nucleation site, or a graphitic layer forms on top of a carbidic layer (i.e. the outer C of the vertical C_2 may become part of the graphite layer, and the inner C may ultimately undergo dissolution into the bulk). In either case, a vertical C_2 serves as the precursor to a nucleation site.

Recently Caputi et al. [5] reported AES and CEELS data for carbon on Ni(100) in the region 520-770 K. Core-level and valence band XPS data have also been reported [5]. A detailed interpretation of the AES and XPS data has revealed extensive C-C bonding on the surface, in what was previously believed to be carbidic (i.e. only C-M bonding) in character [9]. At higher temperatures, just prior to the formation of graphite around 620 K, the amount of C-C bonding appears to decrease. However, no meaningful interpretation of the CEELS data has been reported.

In NEXAFS, the dipole selection rule (i.e. $s \rightarrow p$ only) is appropriate. By CEELS, we mean the use of small electron energies (500-1000 eV) and the measurement of back scattered electrons which have suffered large momentum transfer, in which case the validity of the dipole selection rule is not expected. Thus optically forbidden monopole transitions should be evident. Nevertheless, CEELS data can still be utilized to obtain some of the same information obtainable from NEXAFS data.

We utilize equations derived by Cheung [10] for determining the angular dependence of CEELS data for graphite, which has the σ orbital parallel to the surface (i.e. $\alpha = 90^\circ$ and $\beta = 0^\circ$ as defined above). We obtain:

$$\{1s \rightarrow \pi\} \propto 1.5\xi \sin^2 \delta + 3\nu [\cos^2 \delta - 0.5 \sin^2 \delta] \sin^2 \theta \quad (3)$$

$$\{1s \rightarrow \sigma\} \propto \xi/3 + \nu [1 - 0.5 \sin^2 \delta] - \nu [\cos^2 \delta - 0.5 \sin^2 \delta] \sin^2 \theta \quad (4)$$

where δ is the electron acceptance angle and ξ and ν are the magnitude of the monopole and dipole contributions, respectively. We compare these

expressions with those above for NEXAFS. If we assume $\delta = 90^\circ$ (i.e. that electrons are counted at all acceptance angles; this mimics the NEXAFS data which utilizes the total electron yield or the Auger yield, which is equivalent to all acceptance angles), we obtain

$$\{1s \rightarrow \pi\} \propto 1.5\nu \cos^2 \theta \quad (5)$$

$$\{1s \rightarrow \sigma\} \propto \xi/3 + 0.5\nu + 0.5\nu \sin^2 \theta \quad (6)$$

These expressions have similar $\sin^2 \theta$ and $\cos^2 \theta$ dependences to those above for NEXAFS as expected. Now if we assume $\delta = 16.5^\circ$ (i.e. the appropriate acceptance angle for a cylindrical mirror analyzer and a 500 eV excitation beam as indicated by Cheung [10]), we obtain the expressions

$$\{1s \rightarrow \pi\} \propto 0.12\nu + 2.64\nu \sin^2 \theta \quad (7)$$

$$\{1s \rightarrow \sigma\} \propto \xi/3 + 0.08\nu + 0.88\nu \cos^2 \theta. \quad (8)$$

Notice the switch in $\cos^2 \theta / \sin^2 \theta$ dependence between eqs. 5, 6 and 7, 8. Eqs. 7 and 8, appropriate for this case, is also different from that for NEXAFS, eqs. 1 and 2. Furthermore, Cheung [10] found empirically for graphite with a 500 eV excitation beam that ξ/ν is about 8. Thus in CEELS for $\theta = 90^\circ$ (i.e. electron beam perpendicular to surface, which is generally the case for the data discussed in this work) the π and σ contributions have nearly equal intensity (eqs. 7 and 8 above both give 2.75ν). If the C-C bond is vertical to the surface, we expect a corresponding reversal in the dipole intensity dependencies giving $\{1s \rightarrow \pi\} = 0.08\nu$ and $\{1s \rightarrow \sigma\} = 5.42\nu$. In summary, the CEELS data should give about equal σ and π area intensities for parallel C-C orientation, and be dominated by σ intensity for perpendicular C-C orientation.

Figs. 2b and c compare $-d^2N(E)/dE^2$ K edge CEELS curves for various carbonaceous layers on metals [5,6] along with NEXAFS data for CO/Ni(100) at 670K in 2d [7]. We have also included in Fig. 2a NEXAFS [11] data for

condensed benzene and cyclohexane for comparison to show the presence of similar σ and π C-C features in these molecules and the absence of the C-H features for the carbonaceous layers as expected. All of the carbonaceous layers were prepared by exposure of the Ni surfaces to CO at around 500K, and then heating. The dashed curve in 2b was reported by Rosei et al [6] for a Ni(111) surface upon heating to 500K with an estimated coverage of about 0.3 ML (this is a very crude estimate). The solid curves in b (at 520K) and c (at 620K) were reported by Caputi et al [5]. Although they do not estimate the C coverage, it is believed to be greater than or equal to 1 ML. The NEXAFS curve in (d) was reported by Stohr and Jaeger [7] with incident angle $\vartheta = 20^\circ$. Thus it emphasizes vertical σ bonds. The latter curve corresponds to less than 0.5 ML of "carbide" C on the surface. The K binding energy is about 282.9 eV for a carbide layer on Ni(100) [12]. We have deconvoluted the Caputi data by a 2 eV Gaussian line shape to regain better resolution since it was taken with a large 6 V_{ptp} modulation voltage.

The deconvoluted Caputi data on Ni(100) and the Rosei data on Ni(111) at 500 K are quite similar as expected. They very clearly reveal the characteristic π^*_{CC} and σ^*_{CC} peaks at 285 eV and 293 eV respectively as seen in the NEXAFS data (Figs. 1 and 2a). Since C-M bonds do not produce peaks in this energy range [8], this clearly indicates the presence of C-C bonding on the surface, consistent with the AES and XPS data [9] as indicated above. The similar area intensities of the π^*_{CC} and σ^*_{CC} peaks clearly indicate that the C-C bonds lie flat on the surface. We would assume that these C-C bonds primarily exist as C_n (n = 2,3 etc, with n=2 favored) species on the surface.

The Caputi data at 620K (curve c) reveal dramatic differences from that at 520K. Now the σ^*_{CC} feature dominates with the π^*_{CC} feature nearly

missing. This strongly indicates that the C-C bonds now stand perpendicular to the surface. We believe the σ^*_{CC} feature now arises from C_2 species standing erect on the surface.

NEXAFS data for CO/Ni(100) at 300 K [7] (not shown) clearly show the π^* and σ^* CO bond features. Heating to 670K breaks all C-O bonds, leaving only atomic C on the surface. Notice that in Fig. 2d, no evidence exist for either C-O or C-C bonds. The features at 284 and 288 eV are attributed [8] to nonbonding p_z orbitals (C dangling bonds pointed away from the Ni surface [8,12]) and σ^*_{CM} orbitals bonding the atomic C to the surface. Evidence for these same features also exists in the deconvolved 620K data of Caputi (curve 2c). Comparison with theoretical density-of-state calculations confirms these assignments [8,13].

In summary, our interpretation of the spectroscopic results are consistent with our previous interpretations of the AES and XPS data [9], and with Darling's EMT theoretical results as discussed above [1]. First, the CEELS data do indeed verify that significant horizontal C-C bonding exists on the surface below 600K. We anticipate that this is in the form of C_n . Around 620K, some vertical C_2 is formed along with considerable C_1 (i.e. atomic C). However, the CEELS and NEXAFS data also suggest that vertical C_2 is formed only at higher coverages (it is clearly present in the Caputi data [coverage about 1 ML] but absent in Stohr and Jaeger's NEXAFS data [coverage < 0.5 ML]). At higher coverages, we envisage that some of the C_2 are forced to flip up to make room for the neighboring horizontal C_2 's to dissociate. These vertical C_2 's may then serve as the precursor for the nucleation of graphite, since it would explain the lack of graphite formation from C_2H_4 /Ni(100) (i.e. at low carbon coverages). Further exposure to C_2H_2 at higher temperatures (i.e. producing higher C coverages) does lead to graphite formation on Ni(100)

[12]. Thus we provide the first experimental evidence for vertical C_2 as a precursor for graphite nucleation and corroborate the theoretical EMT [1] results.

REFERENCES

- ¹G.R. Darling, J.B. Pendry, and R.W. Joyner, *Surf. Sci.* **221** (1989) 69.
- ²M.A. Henderson, G.E. Mitchell, and J.M. White, *Surf. Sci.* **203** (1988) 378.
- ³J.A. Horsley, J. Stohr, and R.J. Koestner, *J. Chem. Phys.* **83** (1985) 3146.
- ⁴F. Zaera, D.A. Fischer, R.G. Carr, and J.L. Gland, *J. Chem. Phys.* **89** (1988) 5335.
- ⁵L.S. Caputi, G. Chiarello, and L. Papagno, *Surf. Sci.* **162** (1985) 259.
- ⁶R. Rosei, S. Modesti, F. Sette, C. Quaresima, A. Savoia, and P. Perfetti, *Phys. Rev.* **B29** (1984) 3416.
- ⁷J. Stohr and R. Jaeger, *Phys. Rev.* **B26** (1982) 4111.
- ⁸D.E. Ramaker and F.L. Hutson, submitted to *Phys. Rev. B*.
- ⁹F.L. Hutson, D.E. Ramaker, and B.E. Koel, submitted to *Surf. Sci.*
- ¹⁰T.T.P. Cheung, *Phys. Rev.* **B31** (1985) 4792.
- ¹¹D.A. Outka and J. Stohr, "Chemistry and Physics of Solid Surfaces VII", R. Vanselow and R. Howe, eds. (Springer-Verlag, Heidelberg, 1988), p.20.
- ¹²S.C. Gebhard and B.E. Koel, *Surf. Sci.*, to be submitted.
- ¹³P.J. Feibelman, *Phys. Rev.* **B26** (1982) 5347.

FIGURE CAPTIONS

Fig. 1 C K NEXAFS data for $C_2H_4/Pt(111)$ at a) 90 K and b) 300 K [3] and for $C_2H_4/Ni(100)$ at c) 130 K and d) 180 K [4]. The Pt data [3] were shifted down by 1.5 eV for better alignment with the Ni data [4] and other NEXAFS data [11]. This shift may arise from energy calibration errors or represent a C K binding energy shift on Pt.

Fig. 2 a) C K NEXAFS data for condensed benzene and cyclohexane [11],
b) $-d^2N(E)/dE^2$ C K edge CEELS data for CO/Ni(100) at 500K (dotted line) [5] and CO/Ni(111) at 520K (solid line [6]),
c) CEELS data for CO/Ni(100) at 620K [5], and
d) NEXAFS data for CO/Ni(100) at 670K, but at low coverage [7].

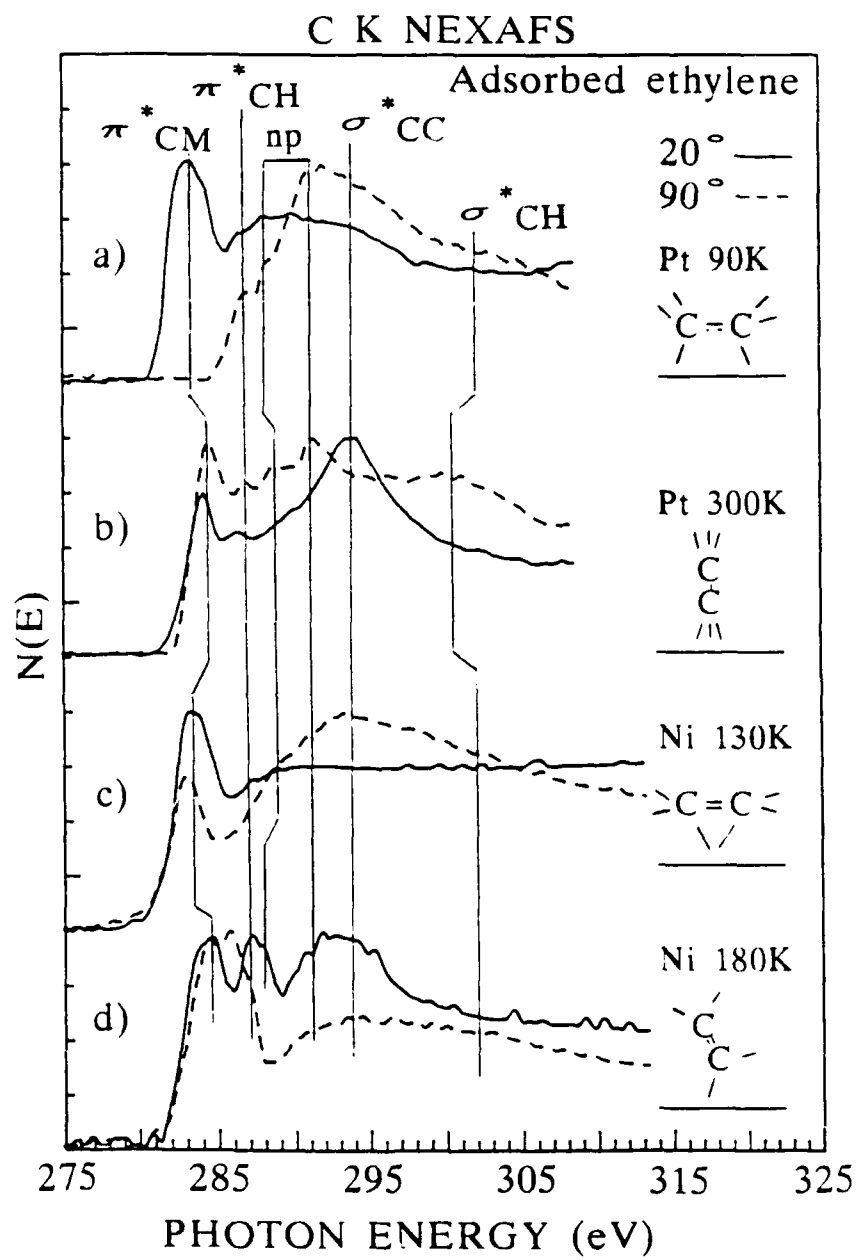


Fig. 1

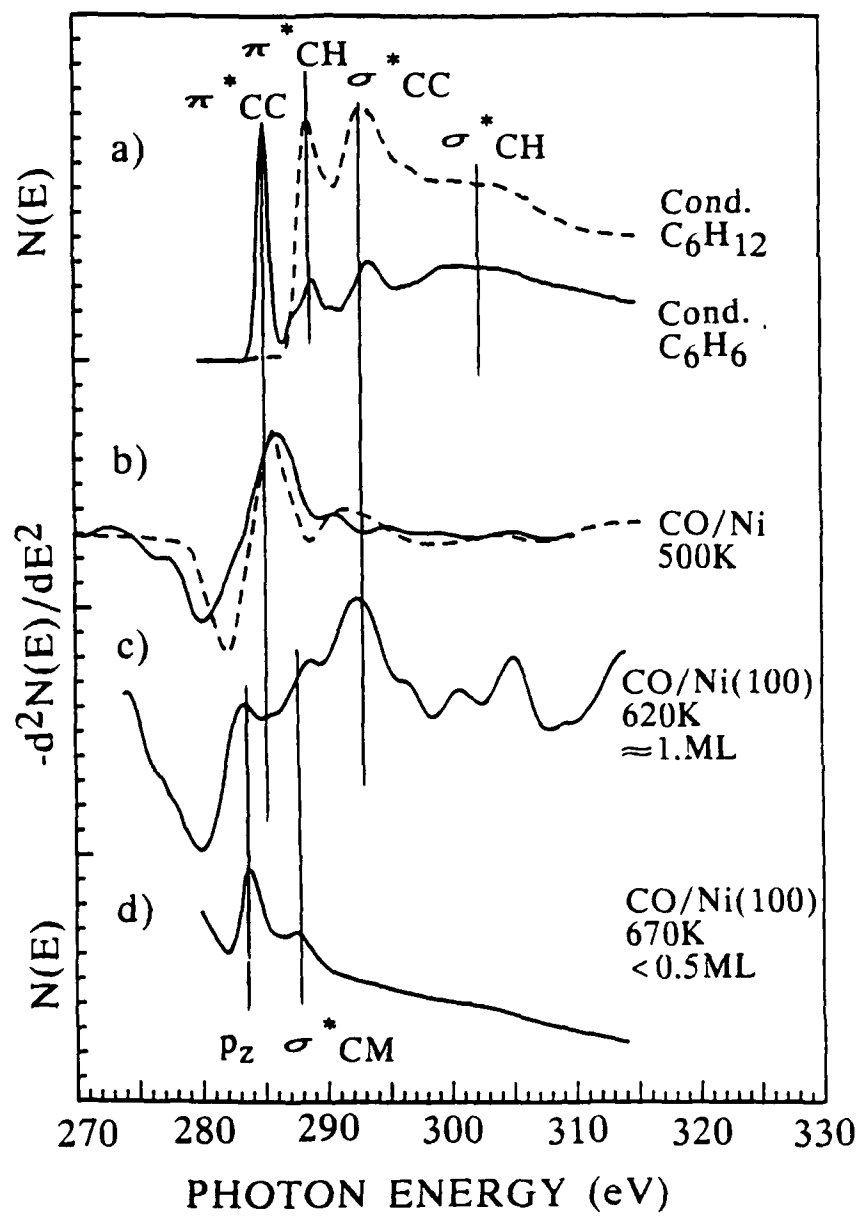


Fig. 2

TECHNICAL REPORT DISTRIBUTION LIST - GENERAL

Office of Naval Research (2)
Chemistry Division, Code 1113
800 North Quincy Street
Arlington, Virginia 22217-5000

Dr. Robert Green, Director (1)
Chemistry Division, Code 385
Naval Weapons Center
China Lake, CA 93555-6001

Commanding Officer (1)
Naval Weapons Support Center
Dr. Bernard E. Douda
Crane, Indiana 47522-5050

Chief of Naval Research (1)
Special Assistant for Marine
Corps Matters
Code 00MC
800 North Quincy Street
Arlington, VA 22217-5000

Dr. Richard W. Drisko (1)
Naval Civil Engineering
Laboratory
Code L52
Port Hueneme, CA 93043

Dr. Bernadette Eichinger (1)
Naval Ship Systems Engineering
Station
Code 053
Philadelphia Naval Base
Philadelphia, PA 19112

David Taylor Research Center (1)
Dr. Eugene C. Fischer
Annapolis, MD 21402-5067

Dr. Sachio Yamamoto (1)
Naval Ocean Systems Center
Code 52
San Diego, CA 92152-5000

Dr. James S. Murday (1)
Chemistry Division, Code 6100
Naval Research Laboratory
Washington, D.C. 20375-5000

Dr. Harold H. Singerman (1)
David Taylor Research Center
Code 283
Annapolis, MD 21402-5067

Defense Technical Information Center
Building 5, Cameron Station
Alexandria, VA 22314

ENCLOSURE(2)

FY90 Abstracts Distribution List for Solid State & Surface Chemistry

Professor John Baldeschwieler
Department of Chemistry
California Inst. of Technology
Pasadena, CA 91125

Professor Paul Barbara
Department of Chemistry
University of Minnesota
Minneapolis, MN 55455-0431

Dr. Duncan Brown
Advanced Technology Materials
520-B Danury Rd.
New Milford, CT 06776

Professor Stanley Bruckenstein
Department of Chemistry
State University of New York
Buffalo, NY 14214

Professor Carolyn Cassady
Department of Chemistry
Miami University
Oxford, OH 45056

Professor R.P.H. Chang
Dept. Matls. Sci. & Engineering
Northwestern University
Evanston, IL 60208

Professor Frank DiSalvo
Department of Chemistry
Cornell University
Ithaca, NY 14853

Dr. James Duncan
Federal Systems Division
Eastman Kodak Company
Rochester, NY 14650-2156

Professor Arthur Ellis
Department of Chemistry
University of Wisconsin
Madison, WI 53706

Professor Mustafa El-Sayed
Department of Chemistry
University of California
Los Angeles, CA 90024

Professor John Eyler
Department of Chemistry
University of Florida
Gainesville, FL 32611

Professor James Garvey
Department of Chemistry
State University of New York
Buffalo, NY 14214

Professor Steven George
Department of Chemistry
Stanford University
Stanford, CA 94305

Professor Tom George
Dept. of Chemistry & Physics
State University of New York
Buffalo, NY 14260

Dr. Robert Hamers
IBM T.J. Watson Research Center
P.O. Box 218
Yorktown Heights, NY 10598

Professor Paul Hansma
Department of Physics
University of California
Santa Barbara, CA 93106

Professor Charles Harris
Department of Chemistry
University of California
Berkeley, CA 94720

Professor John Hemminger
Department of Chemistry
University of California
Irvine, CA 92717

Professor Roald Hoffmann
Department of Chemistry
Cornell University
Ithaca, NY 14853

Professor Leonard Interrante
Department of Chemistry
Rensselaer Polytechnic Institute
Troy, NY 12181

Professor Eugene Irene
Department of Chemistry
University of North Carolina
Chapel Hill, NC 27514

Dr. Sylvia Johnson
SRI International
333 Ravenswood Avenue
Menlo Park, CA 94025

Dr. Zakya Kafafi
Code 6551
Naval Research Laboratory
Washington, DC 20375-5000

Professor Larry Kesmodel
Department of Physics
Indiana University
Bloomington, IN 47403

Professor Max Lagally
Dept. Metal. & Min. Engineering
University of Wisconsin
Madison, WI 53706

Dr. Stephen Lieberman
Code 522
Naval Ocean Systems Center
San Diego, CA 92152

Professor M.C. Lin
Department of Chemistry
Emory University
Atlanta, GA 30322

Professor Fred McLafferty
Department of Chemistry
Cornell University
Ithaca, NY 14853-1301

Professor Horia Metiu
Department of Chemistry
University of California
Santa Barbara, CA 93106

Professor Larry Miller
Department of Chemistry
University of Minnesota
Minneapolis, MN 55455-0431

Professor George Morrison
Department of Chemistry
Cornell University
Ithaca, NY 14853

Professor Daniel Neumark
Department of Chemistry
University of California
Berkeley, CA 94720

Professor David Ramaker
Department of Chemistry
George Washington University
Washington, DC 20052

Dr. Gary Rubloff
IBM T.J. Watson Research Center
P.O. Box 218
Yorktown Heights, NY 10598

Professor Richard Smalley
Department of Chemistry
Rice University
P.O. Box 1892
Houston, TX 77251

Professor Gerald Stringfellow
Dept. of Matls. Sci. & Engineering
University of Utah
Salt Lake City, UT 84112

Professor Galen Stucky
Department of Chemistry
University of California
Santa Barbara, CA 93106

Professor H. Tachikawa
Department of Chemistry
Jackson State University
Jackson, MI 39217-0510

Professor William Unertl
Lab. for Surface Sci. & Technology
University of Maine
Orono, ME 04469

Dr. Terrell Vanderah
Code 3854
Naval Weapons Center
China Lake, CA 93555

Professor John Weaver
Dept. of Chem. & Mat. Sciences
University of Minnesota
Minneapolis, MN 55455

Professor Brad Weiner
Department of Chemistry
University of Puerto Rico
Rio Piedras, Puerto Rico 00931

Professor Robert Whetten
Department of Chemistry
University of California
Los Angeles, CA 90024

Professor R. Stanley Williams
Department of Chemistry
University of California
Los Angeles, CA 90024

Professor Nicholas Winograd
Department of Chemistry
Pennsylvania State University
University Park, PA 16802

Professor Aaron Wold
Department of Chemistry
Brown University
Providence, RI 02912

Professor Vicki Wysocki
Department of Chemistry
Virginia Commonwealth University
Richmond, VA 23284-2006

Professor John Yates
Department of Chemistry
University of Pittsburgh
Pittsburgh, PA 15260